ELSEVIER

NDT&E International 33 (2000) 555–563

NDT&E international

www.elsevier.com/locate/ndteint

Characterization of adhesive bond properties using Lamb waves

K. Heller[a], L.J. Jacobs[a,*], J. Qu[b]

[a]*School of Civil and Environmental Engineering, Georgia Institute of Technology, Atlanta, GA 30332-0355, USA*
[b]*G.W. Woodruff School of Mechanical Engineering, Georgia Institute of Technology, Atlanta, GA 30332-0405, USA*

Received 15 November 1999; revised 20 March 2000; accepted 29 March 2000

Abstract

This research combines laser ultrasonic techniques with the two-dimensional Fourier transform (2D-FFT) to characterize adhesive bond properties. The experimental procedure consists of measuring a series of equally spaced, transient Lamb waves in specimens consisting of aluminum plates joined with an adhesive bond. The frequency spectrum (dispersion curves) for each specimen are obtained by operating on these transient waveforms with the 2D-FFT. This study quantifies the effect of bond stiffness on the dispersion curves of two different bonded specimens (a single aluminum plate with an adhesive transfer tape attached to one side, and two aluminum plates joined with the same adhesive tape) and four adhesive bond conditions (un-aged, and three different aging temperatures and times). The proposed procedure consists of first determining the frequency spectrum of the Lamb waves that propagate in each of the two bonded specimens (plus a single plate); these measurements provide the dispersion curves for each specimen in their un-aged state. Degradation causes changes in the stiffness of an adhesive bond, which causes changes in the dispersion curves of the aged specimens. Experimentally measured dispersion curves are used to quantitatively track changes in the bonded specimens, as a function of age. Finally, these experimental results are interpreted in terms of an analytical model that replaces the adhesive bond layer with a linear spring boundary condition. © 2000 Published by Elsevier Science Ltd.

Keywords: Adhesive bonds; Degradation; Dispersion curves

1. Introduction

The use of advanced structural materials and the ever-present need for performance efficiency (such as low element weight and high strength) has heightened the demand for effective joining methodologies. Adhesive bonds have emerged as a particularly promising technology because of their low weight, low cost and ease of assembly. The increased usage of adhesive joints has created the requirement for more reliable techniques capable of non-destructively characterizing these types of bonds. Unfortunately, conventional ultrasonic methodologies (such as pulse-echo) are ineffective in interrogating large bonded areas. A promising new methodology uses guided Lamb (plate) waves to characterize adhesive bond properties. The primary advantage of using guided waves in this application is that they can quickly and accurately interrogate a large bonded area.

This research combines laser ultrasonic techniques with the two-dimensional Fourier transform (2D-FFT) to characterize adhesive bond properties. The high fidelity, broad bandwidth and non-contact nature of this optical technique are critical for the success of this study. Since laser ultrasonics measures with a point source/point receiver, it permits usage of a spatial sampling technique, the 2D-FFT. By using these state-of-the-art laser ultrasonic methodologies, it is possible to experimentally measure transient Lamb waves in bonded specimens without any of the frequency biases present in, for example, piezoelectric transducers.

This study quantifies the effect of bond stiffness on the dispersion curves of two different specimens, each manufactured with the same adhesive bond—a commercially available, double coated, adhesive transfer tape. Note that this tape cures at room temperature (≈20°C) and has a Young's modulus (elastic stiffness) of 5 MPa. Two bonded specimens are examined: a single aluminum plate with a bond on one side (but not joined to anything)—referred to as the tape specimen; and two aluminum plates joined with an adhesive bond—referred to as the bond specimen. In addition, the dispersion curves of a single aluminum plate are measured to provide a benchmark of the accuracy and robustness of the proposed experimental procedure.

The experimental procedure consists of first determining the frequency spectrum of the Lamb waves that propagate in

* Corresponding author. Tel./fax: +1-404-894-2771/0211.
E-mail address: laurence.jacobs@ce.gatech.edu (L.J. Jacobs).

0963-8695/00/$ - see front matter © 2000 Published by Elsevier Science Ltd.
PII: S0963-8695(00)00022-0

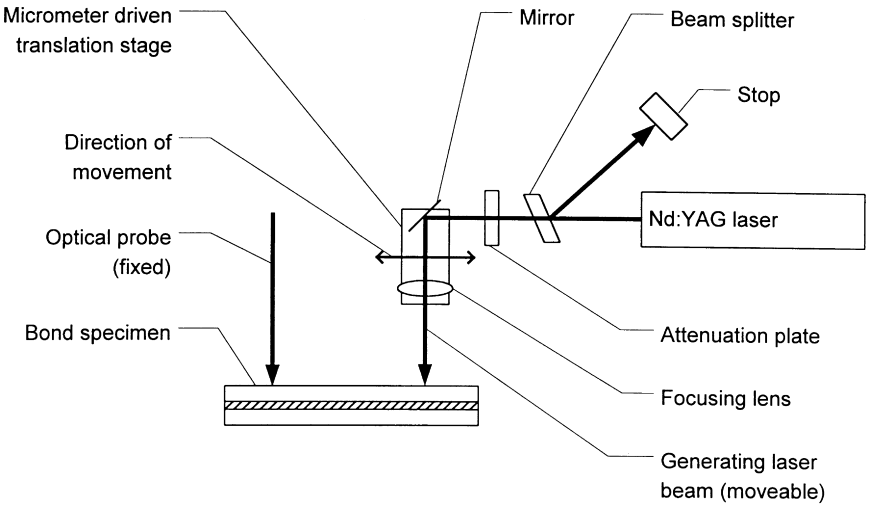

Fig. 1. Schematic of laser generation setup.

each of the two bonded specimens (plus a single plate); these measurements provide the dispersion curves for each specimen in their reference state, un-aged. Degradation (aging in this study) causes changes in the stiffness and microstructure of an adhesive bond, which in turn, should cause changes in the dispersion curves of the aged specimens. As a result, experimentally measured dispersion curves are used to quantitatively track changes in the bonded specimens, as a function of age.

There has been extensive research into the characterization of adhesive bonds (see Thompson and Thompson [1] for a review), but there is less information on guided waves in adhesively bonded structures—especially in the frequency range of this research. Recently, Rose et al. [2] developed dispersion curves for titanium diffusion bonds and examined frequency shifts and spectral peak-to-peak ratios of different bonded states. Achenbach and Parikh [3] performed a theoretical investigation on the non-linear behavior of adhesive bonds. The main focus of their work is reflected and transmitted waves at interfaces. Adler et al. [4] studied guided waves generated with transducers in friction welded aluminum–steel bonds. Delamination in curved bonded aircraft structures is investigated by Rose et al. [5] using energy losses of transient signals. Jungman et al. [6] analyzed interface properties in a three-layer system of a metal plate–epoxy bond–metal plate using leaky Lamb waves. This research reveals that the reflection and transmission coefficients are not very sensitive to the interface properties. Nagy and Adler [7] studied guided waves in adhesive layers between two halfspaces, demonstrating that the resulting dispersion curves are relatively insensitive to the properties of the adhesive layer. Rohklin and Wang [8] examined Lamb waves in lap–shear joints, including the development of an analytical spring model, while Lowe and Cawley [9] analyzed the sensitivity of adhesive bond properties on guided waves using a three-layer model. In addition, a number of researchers have developed dispersion curves using oblique incidence measurements with immersion piezoelectric transducers (e.g. see Mal et al. [10]).

The objective of the present study is to evaluate the effectiveness of combining laser ultrasonic techniques with the 2D-FFT to characterize adhesive bond properties. The experimental procedure consists of measuring a series of equally spaced, transient Lamb waves in bonded specimens and then operating on these transient waveforms with the 2D-FFT to develop the specimen's frequency spectrum (dispersion curves). These experimentally measured dispersion curves are then used to quantitatively characterize the condition of the adhesive bond, as a function of degradation. As a final step, the experimentally observed behavior is interpreted using an analytical model.

2. Experimental procedure

The Nd:YAG laser (1064 nm) used for generation emits a 450 mJ, 4–6 ns pulse, and this beam is attenuated and focused before it strikes the specimen. The focusing lens and alignment mirror are mounted on a (micrometer driven) translation stage that allows for precise (horizontal) movement of the optical source (see Fig. 1). This setup provides a laser source that generates exactly the same ultrasonic signal, at multiple, equally spaced locations, throughout each test. Note that this setup does not guarantee that the laser source is exactly the same (spot size of approximately 1 mm) for all the specimens (or for a specimen that is removed and re-installed), just that the laser source remains constant as the source is translated to different spatial locations on the same specimen. Laser detection of these ultrasonic (Lamb) waves is accomplished with a heterodyne interferometer [11] that uses the Doppler shift to measure out-of-plane surface velocity (particle velocity) at a point on the specimen's surface. The interferometer makes high-fidelity, absolute measurements of surface velocity (particle

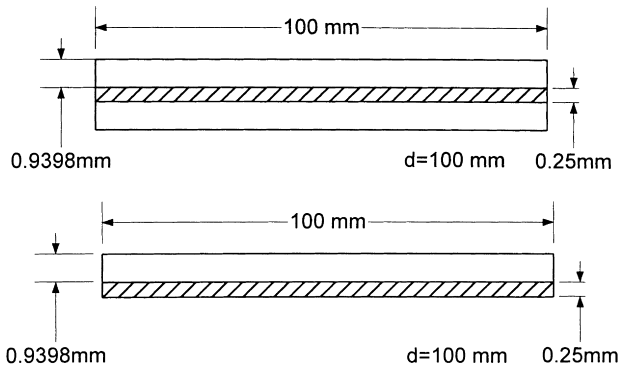

Fig. 2. Bond specimen (upper) and tape specimen (lower).

velocity) over a bandwidth from 200 kHz to 10 MHz. Note that all of the waves presented are low-pass filtered at 10 MHz. In addition, each waveform presented represents a collection of averages, sometimes as many as one hundred. This signal averaging procedure works because noise is random, while the "real" signal is repeatable; signal-to-noise ratio (SNR) is improved by the square root of N, where N is the number of averages.

The adhesive material employed in this research is used in high-performance joint applications and is capable of replacing rivets, spot welds and many other fasteners. The great advantage of tape technology is its ease of applicability and the guarantee of uniformly bonded connections. The tape is manufactured by the 3M Company (Adhesive Transfer Tape F-9473PC), and 3M provides the following material properties: bond thickness $t = 0.25$ mm; Young's modulus $E = 5$ MPa; Poisson's ratio $\nu = 0.5$; short-term temperature tolerance of 260°C; and long-term temperature tolerance of 149°C [12].

The two bonded specimens considered in this study are identified as the tape specimen and the bond specimen (Fig. 2). The tape specimen is a single (aluminum) plate with adhesive transfer tape attached to one side, while the bond specimen consists of two of the same single plates, bonded together with the same adhesive tape. The plates are 3003 aluminum, with thickness $t = 0.9398$ mm and dimensions 100×100 mm. Note that a single aluminum plate (identical to the plates used in the bonded specimens) is also investigated.

Four different bond conditions are investigated:

- un-aged condition—original condition;
- condition 1—specimen heated for 3 h at 170°C;
- condition 2—condition 1, followed by heating for 4 h at 285°C;
- condition 3—specimen heated for 4 h at 285°C.

Since the temperature of condition 1 is only slightly above the adhesive tape's long-term tolerance, this temperature only causes physical aging of the tape material, a reversible damage process. In contrast, conditions 2 and 3 damage the adhesive bond irreversibly—they induce chemical aging in the adhesive material, an irreversible change.

3. Experimental results and discussion

While the receiver is kept in a fixed position, the source is placed at 50 equally spaced locations. Incremental (Δx) distances of 0.30 mm (or 0.40 mm in some cases) separate these multiple source locations. Note that the closest source-to-receiver (propagation) distance is approximately 30 mm. This results in the generation and detection of 50 waveforms, each with a different propagation distance and each generated with exactly the same source.

Fig. 3 shows three typical transient waveforms with the same propagation distance (47.5 mm), but measured in the three different specimens (the tape specimen, the bond specimen and the single plate). Note that the trigger time of these waveforms corresponds to the "spike" at ≈ 5 μs; this spike is caused by the electromagnetic discharge of the Nd:YAG laser, but the system is actually triggered by a repeatable voltage output coincident with the laser's firing. Consider the outstanding SNR exhibited in these waveforms; high SNR is critical for the success of the next step—development of dispersion curves. A qualitative analysis of these three waveforms shows identical arrival times for the beginning of the signal (the first non-zero disturbance at ≈ 13 μs) and no significant differences between the shape of each bonded specimen signal, while the shape of the single plate signal is very different. The single plate shows more "signal content" (higher amplitude content before and after the arrival of the Rayleigh wave at ≈ 20 μs). In addition, the first reflections from the specimens' edges are visible (e.g. at ≈ 37 μs in the bond specimen). Unfortunately, besides making these generic comments about differences in shape, no other analysis is possible—it is impossible to quantitatively interpret these transient waveforms. However, it is possible to develop dispersion curves and then quantitatively interpret these results.

This study uses the 2D-FFT to operate on this set of (50) equally spaced, transient waveforms and develops dispersion curves for each specimen. Implementation of the 2D-FFT is fairly straightforward—perform a temporal Fourier transform (from the time to the frequency domain) followed by a spatial Fourier transform (spatial to the wavenumber domain) [13,14]. The resulting frequency (f) versus wavenumber (k) spectrum shows a series of peaks that represent individual modes. Note that the signals are windowed to remove any edge reflections—since the arrival of any reflections from the edges occur after the portion of interest, these reflections are removed so the specimens are considered to be infinite plates.

To demonstrate the accuracy of the proposed 2D-FFT procedure, consider the dispersion results for the single

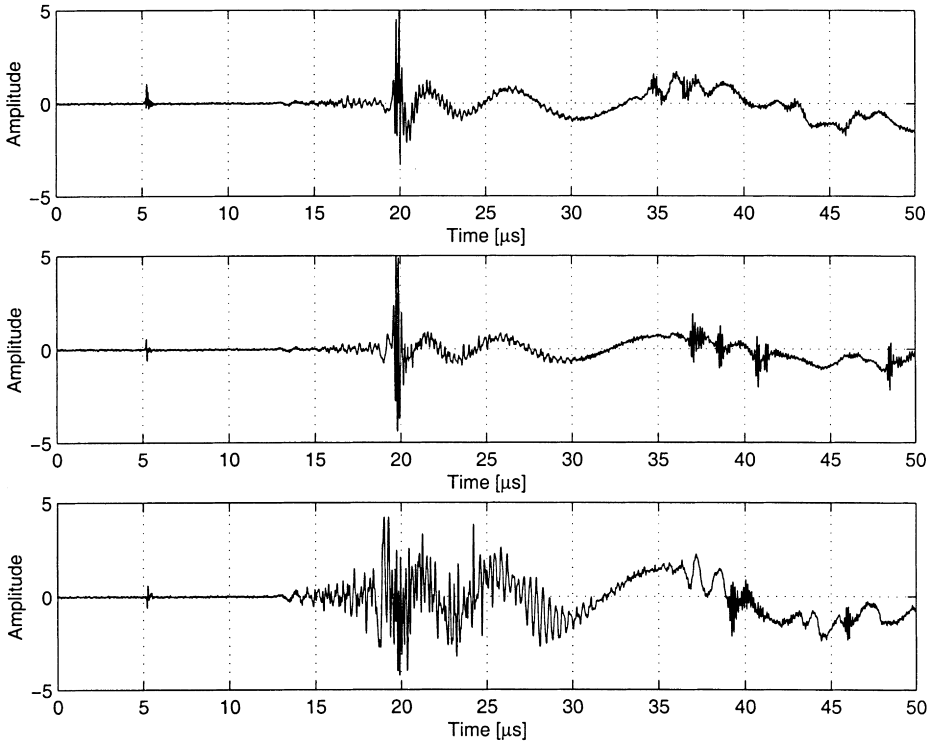

Fig. 3. Comparison of three typical transient waves with the same propagation distance (47.5 mm), but measured in the tape specimen, the bond specimen and the single plate (top, middle and bottom, respectively).

aluminum plate ($t = 0.9398$ mm). Although these dispersion curves are not directly related to the assessment of different bond conditions, they are helpful in interpreting the tape and bond specimen results. Fig. 4 is a contour plot of the three-dimensional frequency versus wavenumber spectrum for the aluminum plate (experimentally measured) superimposed on the theoretical solution (the solid lines) of the Rayleigh–Lamb frequency equations [15]. Fig. 4 indicates that certain k–f combinations have significant amplitudes (peaks), and these combinations are solutions to the plate's dispersion relationship (the plate's individual modes) that exactly match the theoretical solution. The lowest (first from bottom to top) "mountain range" in Fig. 4 represents the first antisymmetric mode, while the next set of peaks (in order of increasing frequency) is the first symmetric mode. Note that these two modes asymptotically approach the Rayleigh phase velocity above $k = 8000$/m (approximately). There are five more modes with lower peaks at higher frequencies; these are the higher modes that carry less energy. Note that the higher modes have clear and definitive cut-off frequencies, indicating that these higher modes only exist above a specific lower frequency value. Dispersion is clearly visible in all of the modes; they follow a curve in the beginning, and turn into straight lines at higher wavenumbers (or frequencies).

Fig. 4 shows that there are a total of seven experimentally "measurable" modes, through a bandwidth up to 10 MHz (wavenumber up to 10,000/m), and these modes are in excellent agreement with the theoretical solution. This single plate information defines the upper limit of the proposed experimental procedure—if certain modes are not clearly visible in the experimental dispersion curves of a single plate, they will probably not be observed in the tape and bond specimens. If the tape and bond specimens behave like a single, stress free plate (see Section 4 for a discussion), their dispersion curves should not possess more detail than present in the single plate results shown in Fig. 4.

Now consider the dispersion curves of a typical tape specimen, shown in Fig. 5(a). This tape specimen enables an investigation into the behavior of a "plate-like" specimen, but with a different boundary condition on one side than the single plate of Fig. 4—this is an intermediate step between the single plate and the bond specimens. Note that the theoretical dispersion curves for a single plate (solution of the Rayleigh–Lamb equations for $t = 0.9398$ mm) are again plotted as solid lines. Fig. 5(a) contains five modes (possibly six modes, counting the peak above 9 MHz and 8000/m as a barely measurable mode) of a single plate (two modes less than shown in Fig. 4) but they are considerably different in appearance than in Fig. 4. The tape specimen modes are notably less distinct (they are fuzzier) and not as well shaped. More importantly, large parts of all modes have disappeared, when compared to the single plate—the tape modes do not exist through as large a k–f range as the single plate. However, all the tape specimen modes still fit perfectly to the theoretically calculated dispersion curves of a single plate. In summary, the addition of the adhesive tape to a single plate does not cause any frequency shifts in the

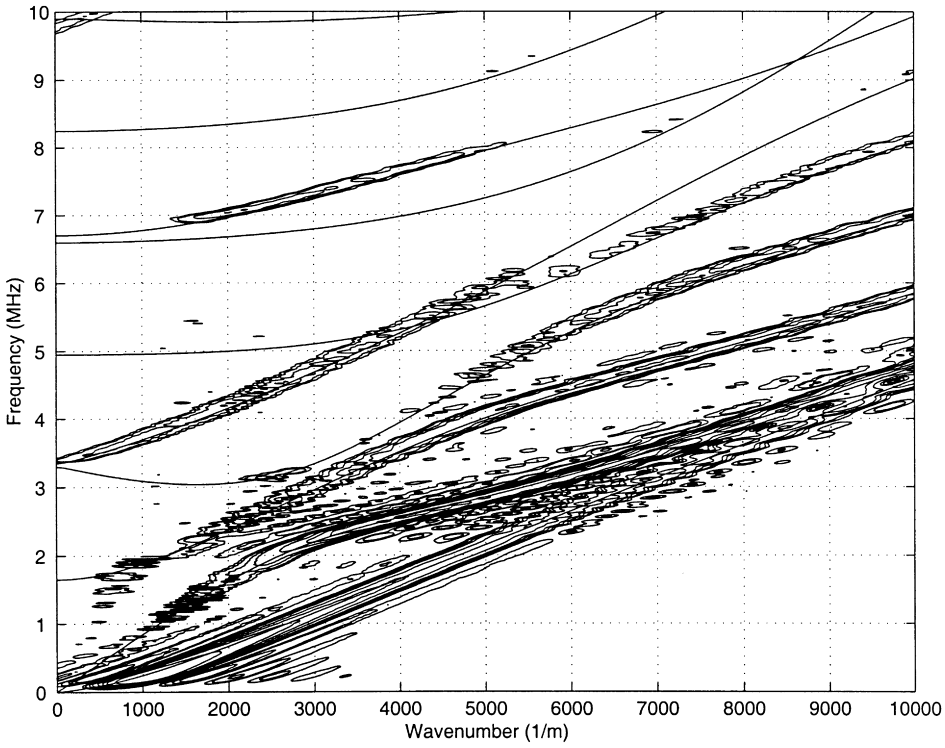

Fig. 4. Contour plot of the frequency versus wavenumber spectrum of a single plate ($t = 0.9398$ mm), with the theoretical solution of the Rayleigh–Lamb frequency equations (solid lines).

dispersion curves, but the tape does "damp-out" portions of the modes, entirely removing at least one mode.

Fig. 5(b) shows the dispersion curves of the same tape specimen as in Fig. 5(a), but aged to condition 3. The most important feature of the dispersion curves of the tape specimen in condition 3 is that modes (especially in the higher frequency regions) present in the un-aged state, vanish with aging. Note that condition 3 ages the bond specimen at a very high temperature, in relation to the adhesive's specified temperature tolerance, so chemical aging occurs. Since the higher frequency modes that are present in the tape specimen's un-aged state disappear, the irreversible damage associated with the chemical aging of this adhesive bond must be responsible for these experimentally observable changes in the tape specimen's dispersion curves. Note that this trend of vanishing modes is not an artifact of the experimental measurements, nor is it caused by changes in the aluminum plate (that could theoretically occur during the aging to condition 3). This fact is verified with a procedure where the tape is removed (with a chemical solvent) from the aluminum plate of a tape specimen that has been aged to condition 3, and the measurements are repeated. The resulting dispersion curves are exactly the same as a single plate shown in Fig. 4 (see Ref. [16] for details).

Now consider the bond specimens; Fig. 6(a) shows the dispersion curves of a typical bond specimen in the un-aged condition and the theoretical dispersion curves for a single plate ($t = 0.9398$ mm) are again plotted as solid lines. Fig. 6(a) shows five modes of a single plate (two less than shown in Fig. 4) and they are well shaped and clearly distinguishable. First, notice that the dispersion curves of the un-aged bond specimen are much more distinct (sharper) in comparison to the un-aged tape specimen (Fig. 5(a)). Next, note that these bond specimen modes correspond to the modes of a single plate ($t = 0.9398$ mm) and not to the modes of a (perfectly bonded) plate with thickness equal to the sum of its two constituent single plates ($2t = 1.8796$ mm). This means that in the un-aged condition, the two plates of the bond specimen act independently of each other, as far as the dispersion curves are concerned. This independence is further verified by making measurements with the detection interferometer (optical probe) on the opposite (as opposed to the same) side of the generation source; the source and receiver on the same side is the configuration used for all results presented in this paper (see Fig. 1). Each of these measurement configurations gives the same results—the dispersion curves shown in Fig. 6(a) [16]. This is interesting, since even though the adhesive bond layer does not "link" the dispersion behavior of each individual plate component, the adhesive bond can transfer enough "energy" to excite guided waves in the opposite plate. Finally, spatial aliasing is shown in the straight line (non-dispersive) peak that appears near 7 MHz. This peak is the spurious continuation of the intersection of the first symmetric and antisymmetric modes at higher wavenumbers; its slope is the Rayleigh phase velocity. This spurious peak appears in this set of dispersion curves (and not in any of the previous ones) because this measurement uses a spatial step size (Δx) of

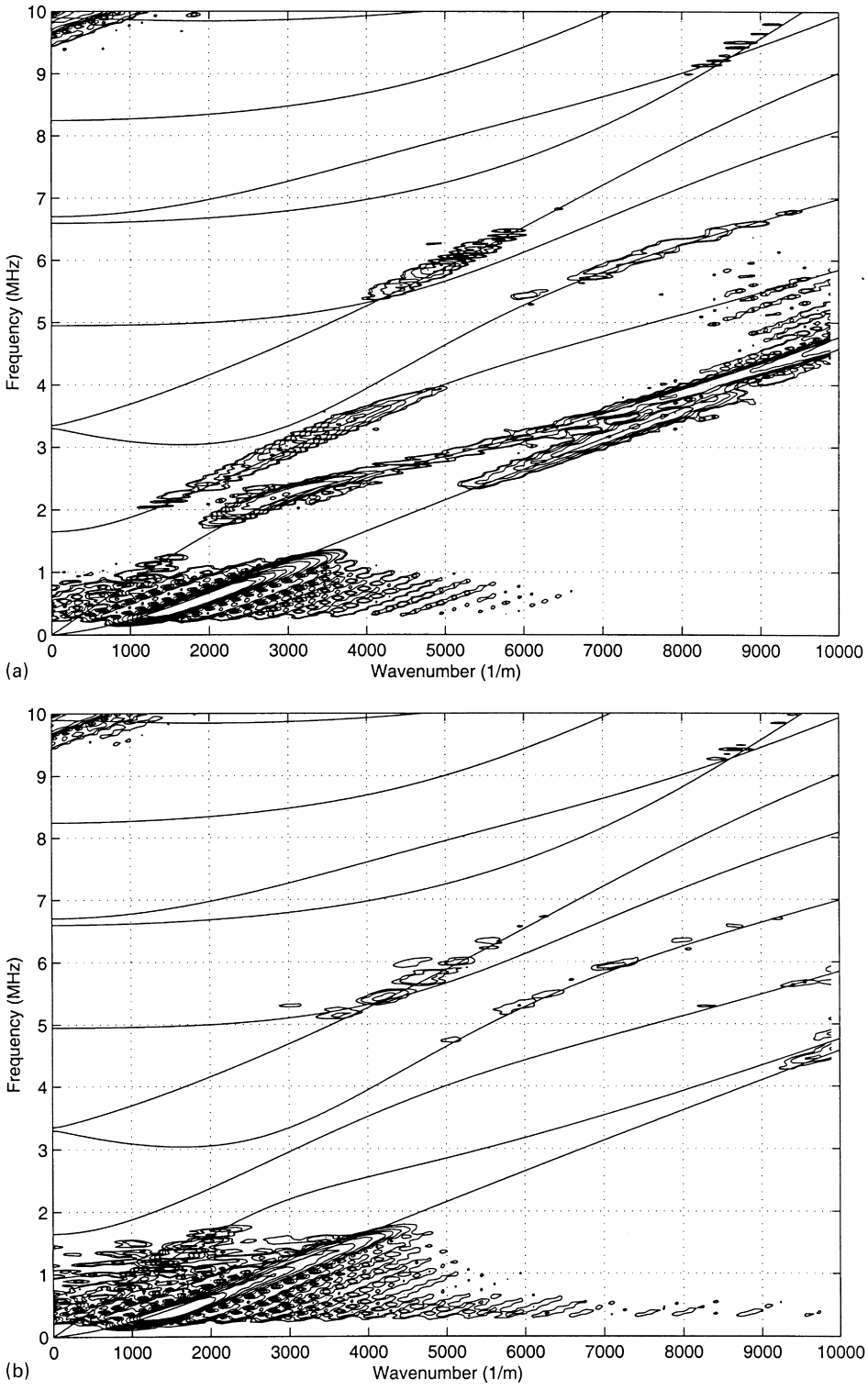

Fig. 5. (a) Contour plot of the frequency versus wavenumber spectrum of an un-aged tape specimen, with the theoretical solution of the Rayleigh–Lamb frequency equations (solid lines) of a single plate ($t = 0.9398$ mm). (b) Contour plot of the frequency versus wavenumber spectrum of same tape specimen in condition 3, with the theoretical solution of the Rayleigh–Lamb frequency equations (solid lines) of a single plate ($t = 0.9398$ mm).

0.40 mm (as opposed to 0.30 mm for the previous measurements), and the spatial "Nyquist wavenumber" ($\pi/\Delta x$) for a 0.40 mm step size is 7854/m (as opposed to 10,472/m for a 0.30 mm step). As a result, the maximum wavenumber shown in Fig. 6(a) is 7854/m—Fig. 6(a) is plotted to 8000/m, while all of the other figures (which use a 0.3 mm step) are plotted to 10,000/m.

The bond specimen of Fig. 6(a) is first aged to condition

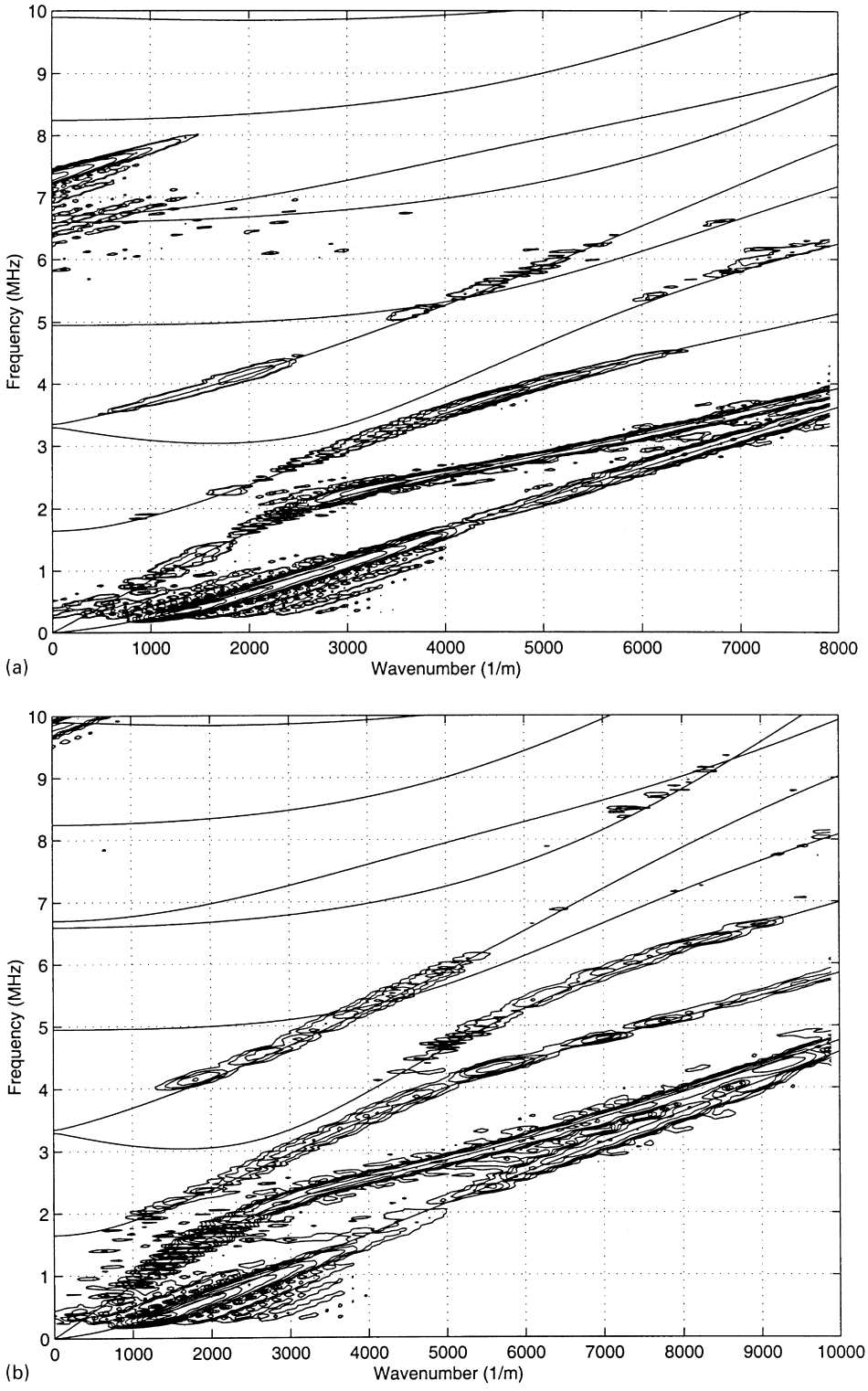

Fig. 6. (a) Contour plot of the frequency versus wavenumber spectrum of an un-aged bond specimen, with the theoretical solution of the Rayleigh–Lamb frequency equations (solid lines) of a single plate ($t = 0.9398$ mm). (b) Contour plot of the frequency versus wavenumber spectrum of the same bond specimen in condition 1, with the theoretical solution of the Rayleigh–Lamb frequency equations (solid lines) of a single plate ($t = 0.9398$ mm). (c) Contour plot of the frequency versus wavenumber spectrum of the same bond specimen in condition 2, with the theoretical solution of the Rayleigh–Lamb frequency equations (solid lines) of a single plate ($t = 0.9398$ mm).

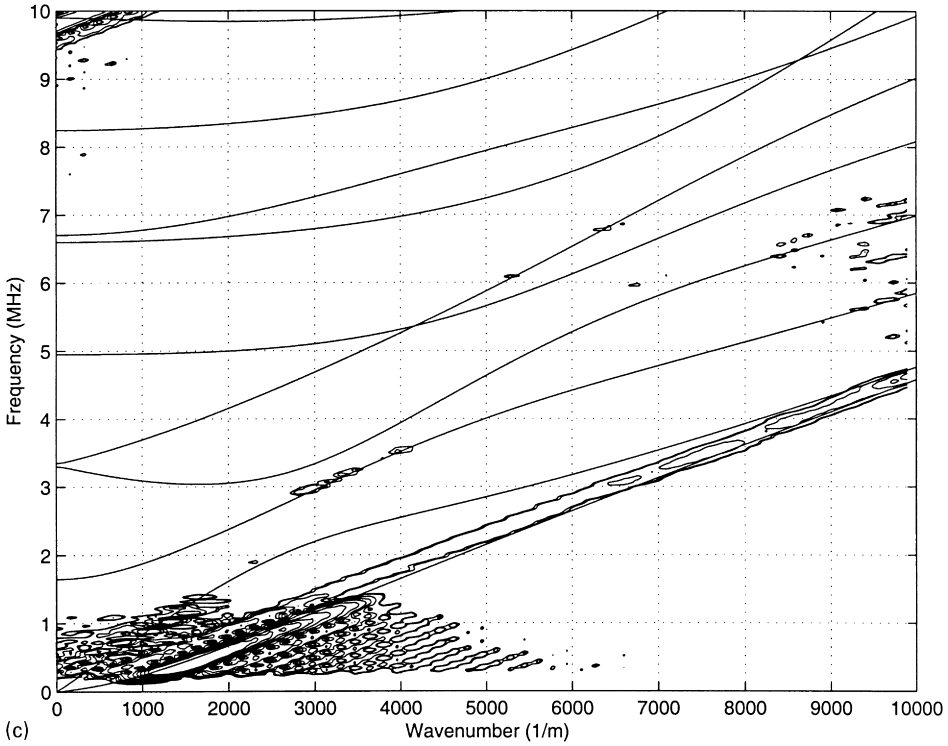

Fig. 6 (*continued*)

1, and then to condition 2, see Fig. 6(b) and (c). The most obvious trend in Fig. 6(a)–(c) is that the modes measured in all conditions fit the modes of a single plate of thickness $t = 0.9398$ mm (the solid lines); the aged bond specimens behave like a single plate, no matter how they are aged. Consider the transition from un-aged to condition 1—the spectrum shown in Fig. 6(b) is not that different from the spectrum in Fig. 6(a). Even after aging to condition 1, the bond specimen behaves in a similar fashion to the un-aged condition. The lower aging temperatures (in relation to the adhesive's specified temperature tolerance) of condition 1 only physically ages the adhesive bond, a reversible process that does not permanently change the bond properties. In contrast, the irreversible damage of chemical aging (associated with condition 2) causes most of the modes that are present in the un-aged and condition 1 states to vanish in condition 2. There is a dramatic difference between Fig. 6(a)–(b) and Fig. 6(c), especially when noting that the straight line peak just above the first theoretical mode (the first antisymmetric) in Fig. 6(c) is the non-dispersive "mode" of a pure shear wave. This peak is hidden in all of the other figures by either the sidelobes (from the 2D-FFT) of the large amplitude first mode (the most common case), or this shear peak has such a small amplitude that it is on the same level as the experimental noise—this is often true for aged specimens, such as the tape specimen in Fig. 5(b). By comparing Figs. 5(b) and 6(c), it is clear that the trend of vanishing modes with increasing bond degradation is present in both the tape and bond specimens. Finally, it is evident that modes disappear with aging, no matter which aging path—un-aged to condition 1 to condition 2, or un-aged to condition 3—is taken. A total of six bond specimens and two tape specimens are tested, and they all show the same trends demonstrated in Figs. 5 and 6 [16].

4. Analytical spring model for the bond specimen

Previous researchers (e.g. Xu and Datta [17] and Mal [18]) developed analytical spring models to explain the behavior of guided waves in bonded plates. In a similar fashion, an additional portion of this research develops an analytical model of the bond specimen (shown in Fig. 2) by considering the two plates and connecting springs (adhesive bond layer) as a single waveguide—one wavenumber–frequency (characteristic) equation for the entire bond specimen (see Ref. [16] for details).

When the spring constants are calculated using the elastic properties provided by 3M [12], this analytical spring model predicts dispersion curves that correspond exactly to those of a 0.9398 mm thick aluminum plate [16]. This verifies the experimentally observed behavior of an un-aged bond specimen in Fig. 6(a). The adhesive layer is relatively flexible, so the dispersion curves for the bond specimen are identical to those for a single plate (adherend)—the bond specimen behaves like a single plate of the thickness of the independent adherends. Note that a similar behavior is observed in Refs. [7,9]. Since the bond specimen dispersion

curves are insensitive to the properties of the adhesive, no frequency shifts are observed in the aged bond (and tape) specimens.

Finally, note that this analytical spring model does not solve for amplitudes; the solution of the characteristic equation only provides a relationship between frequency and wavenumber. As a result, this spring model cannot be used to validate the experimentally observed changes in amplitudes (disappearance of modes), as a function of damage.

5. Conclusions

This research clearly demonstrates the effectiveness of combining laser ultrasonic techniques with the 2D-FFT to characterize the condition of adhesive bonds. By using this innovative technique, it is possible to experimentally measure transient Lamb waves in two types of bonded aluminum plate specimens and to study the influence of the condition of the adhesive material on the dispersion curves of these specimens; this dispersion information is used to monitor changes in bond condition as a function of damage (age in this study). It is critical to note that these experimental measurements are only possible because of the high-fidelity, broadband, point source/point receiver and non-contact nature of laser ultrasonics.

The experimental results show a behavior that is consistent with the trends predicted by an analytical spring model—the modes excited and measured in the bond specimens are always identical to the dispersion curves of a single plate. More importantly, the number of modes measured in a bond specimen is always less than the number of modes measured in a single, stress free plate; they both behave like a single plate, there are just fewer modes observed in a bond specimen. In addition, the modes measured in a bond specimen are less defined (less clarity), and generally exist through a smaller frequency (or wavenumber) bandwidth, than those measured in the corresponding single plate. This decrease in dispersion curve amplitude cannot be predicted (or validated) with the spring model; this analytical spring model only provides the relationship between frequency and wavenumber, and gives no amplitude information. Finally, an important and promising trend is detected when a bond specimen is aged at a very high temperature. When a bond is damaged by chemical aging (the irreversible damage that occurs at these high temperatures), the higher frequency modes that are present in a bond specimen's un-aged state disappear. The irreversible damage associated with chemical aging of an adhesive bond causes a consistent, experimentally observable change in a bond specimen's dispersion curves. As a result, there is the potential to develop a procedure that uses changes in a bond specimen's dispersion curves to monitor adhesive bond stiffness.

Acknowledgements

This work is partially supported by NASA through Grant NAG-1-1810. The Deutscher Akademischer Austausch Dienst (DAAD) provided partial support to Kai Heller.

References

[1] Thompson RB, Thompson DO. Past experiences in the development of tests for adhesive bond strength. Journal of Adhesion Science and Technology 1991;5(8):583–99.
[2] Rose JL, Zhu W, Zaidi M. Ultrasonic NDT of titanium diffusion bonding with guided waves. Materials Evaluation 1998;56(4):535–9.
[3] Achenbach JD, Parikh OK. Ultrasonic analysis of nonlinear response and strength of adhesive bonds. Journal of Adhesion Science and Technology 1991;5(8):601–18.
[4] Adler L, Billy M, Quentin G. Evaluation of friction-welded aluminum–steel bonds using dispersive guided modes of a layered substrate. Journal of Applied Physics 1990;68(12):6072–6.
[5] Rose JL, Rajana KM, Hansch MKT. Ultrasonic guided waves for NDE of adhesively bonded structures. Journal of Adhesion 1995;50:71–82.
[6] Jungman A, Guy P, Quentin G. Characterization of glued bonds using ultrasonic reflected beam. Review of Progress in Quantitative Nondestructive Evaluation 1991;10B:1319–27.
[7] Nagy PB, Adler L. Nondestructive evaluation of adhesive joints by guided waves. Journal of Applied Physics 1989;66(10):4658–63.
[8] Rohklin SI, Wang YJ. Analysis of boundary conditions for elastic wave interaction with an interface between two solids. Journal of the Acoustical Society of America 1991;89(2):503–15.
[9] Lowe MJS, Cawley P. The applicability of plate wave techniques for the inspection of adhesive and diffusion bonded joints. Journal of Nondestructive Evaluation 1994;13(4):185–200.
[10] Mal AK, Xu PC, Bar-Cohen Y. Analysis of leaky Lamb waves in bonded plates. International Journal of Engineering Science 1989;27(7):779–91.
[11] Bruttomesso DA, Jacobs LJ, Costley RD. Development of an interferometer for acoustic emission testing. Journal of Engineering Mechanics 1993;119(11):2303–16.
[12] Designer's reference guide to adhesive technology. St. Paul, MN: 3M Adhesives Division, 1995.
[13] Alleyne D, Cawley P. A two-dimensional Fourier transform method for measurement of propagating multimode signals. Journal of the Acoustical Society of America 1991;89(3):1159–68.
[14] Eisenhardt C, Jacobs LJ, Qu J. Application of laser ultrasonics to develop dispersion curves for elastic plates. Journal of Applied Mechanics 1999;66(4):1043–5.
[15] Mindlin RD. Waves and vibrations in isotropic, elastic plates. Structural Mechanics, Proceedings of the First Symposium on Naval Structural Mechanics, 1958. p. 199–232.
[16] Heller KS. Laser generated and detected Lamb waves to characterize adhesive bond properties. Studienarbeit Thesis, Institute A of Mechanics, University of Stuttgart, 1999.
[17] Xu PC, Datta SK. Guided waves in a bonded plate: a parametric study. Journal of Applied Physics 1990;67(11):6779–86.
[18] Mal AK. Guided waves in layered solids with interface zones. International Journal of Engineering Science 1988;26(8):873–81.